Complex Oscillatory Behavior of the Mercury Beating Heart System

Susana Castillo-Rojas,[†] **Guillermina Burillo,**[†] **and Luis Vicente**[*,‡]

Instituto de Ciencias Nucleares, UNAM, Apartado Postal 70-543, Circuito Exterior CU, 04510 México, D. F., México, and Departamento de Física y Química Teórica, Facultad de Química, UNAM, 04510 México, D. F., México, vicente@eros.pquim.unam.mx

Received February 12, 2002. Accepted April 5, 2002

Abstract: We show the dynamics of the oscillatory Mercury Beating Heart (MBH) reaction in acid aqueous solution with $[Ce^{IV}(SO_4)_3]^{2-}$ as oxidizing agent. The rich dynamics is appropriate to introduce students to oscillatory chemical reactions and nonlinear concepts. These oscillations display different modes of oscillations with geometric structures similar to heart, circle, and pointed stars. We consider oxidation–reduction reactions to explain the different periods of oscillations due mainly to the formation of mercury(I) species and plot the so-called reconstruction attractors from the variation of the Hg electrode potential in time.

Introduction

Oscillations in chemistry have been known as isolated observations since the XIX century [1]. One of the first, more completely reported of these was the oscillatory reaction in a homogeneous system discovered in 1917 by Bray and Caulkins, the decomposition of H_2O_2 in acid medium catalyzed by IO_3^- ions. The light absorption by I_2 shows oscillatory behavior, which is not sustained if the reaction is performed in a closed reactor. A new era began in the 1960s when Zhabotinsky [2] showed irrefutable evidence of oscillations in the reaction discovered by Belousov. The redox reaction known as the Belousov–Zhabotinsky (BZ) reaction can be carried out for long periods of time using open reactors, which is necessary for quantitative measure and understanding.

A different phenomenon in which oscillatory motion is induced by chemical reactions at interfaces was observed long ago. It happens when an iron needle is put into contact with a mercury drop containing an acid solution of an oxidizer. The so-called Mercury Beating Heart (MBH) system was observed by Kühne and reported by Lippmann as early as 1873 [3, 4].

The MBH is a classical experiment done in classroom demonstrations and involves a complex network of redox reactions coupled with hydrodynamic motion of the mercury drop, but only recently has it been the subject of detailed measurements aimed to understand the mechanism of the oscillations [5–9]. Keizer et al. [5] were the first to make a detailed analysis of this reaction with the system functioning like an electrochemical cell. They put a tungsten electrode in contact with the Hg and attaching it to an Al or Fe counter electrode set the potential of this tungsten electrode. The oscillatory behavior of the voltage between Hg and the corroding electrode is then followed on an oscilloscope. In acidic oxidizing solutions they associated the oscillations with the formation and removal of a Hg_2SO_4 surface layer and, in the absence of strong oxidants, it was found that the presence of O_2(aq) is responsible for the modifications in surface tension of the Hg drop.

Olson et al. [7] have introduced a reference electrode that allows the Hg electrode potential to be followed. They showed that in neutral and basic solutions oscillations could be sustained by application of an external oscillating field without formation of a surface film. In general all these papers have reported only on basically three modes of oscillations: breather, two-fold, and three-fold (Figure 1). Recently [11], we have reported different modes of oscillations and the transitions between them from the viewpoint of nonlinear systems. It is our purpose to show here that the MBH system is suitable for the study of chemical oscillations and concepts in nonlinear chemical kinetics as an introduction of nonlinear systems in chemistry in an undergraduate environment. In this way we give in the next section a detailed account of the experimental setup. In Section 3 we consider the mechanism and in Section 4 we make use of the concepts of nonlinear dynamics applied to the MBH system. Finally in Section 5 we give our conclusions.

The Experiment

All solutions used in the experiment were made from reagent chemicals. A volume of 8 mL of metallic Hg was placed in a (concave) porcelain dish of 385-mL capacity, which contained 25 mL of 6 M sulfuric acid. A 0.1 M $Ce(SO_4)_2$ solution was prepared in 6 M sulfuric acid and standardized with sodium oxalate by inverse volumetric titration. At this concentration of sulfuric acid the major cerium species is [9] $[Ce^{IV}(SO_4)_3]^{2-}$ and it acts as the oxidant agent. The ceric sulfate dissolves according to

$$Ce(SO_4)_2 + SO_4^{2-}(aq) \rightleftarrows [Ce^{IV}(SO_4)_3]^{2-} \qquad (1)$$

In our experiment a fixed volume (4.65 mL) of titrated oxidant solution was added to the sulfuric acid contained in the porcelain dish to obtain a final concentration in $[Ce^{IV}(SO_4)_3]^{2-}$ of around 15.5×10^{-3} M and the solution was shaken initially manually for 1 min. Within this concentration it is possible to observe the different dynamical modes referred to in this work. More precisely, only for concentrations in the range 13.8 to 15.5×10^{-3} M the initial aperiodic

---

[*] Address correspondence to this author.

[†] Instituto de Ciencias Nucleares

[‡] Departamento de Física y Química Teórica

S1430-4171(02)03558-4, Published on Web 05/10/2002, 10.1007/s00897020558a, 730159lv.pdf

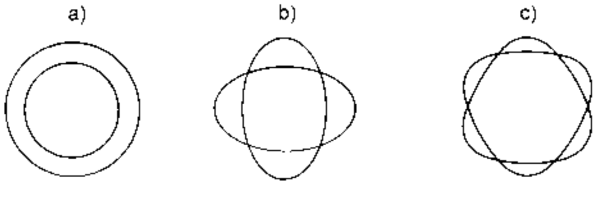

Figure 1. Different modes of oscillations: (a). concentric breathing, (b) two-fold, and (c) triangular heart-shaped or three-fold. There is an alternation between the two superimposed shapes.

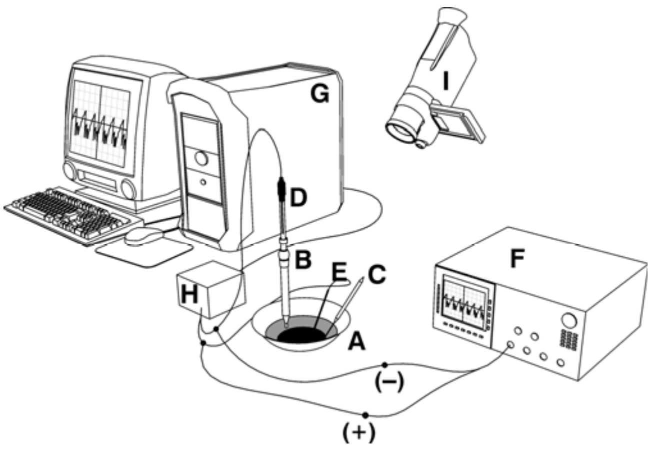

Figure 2. Experimental setup: (A) porcelain dish, (B) salt bridge, (C) iron tip, (D) saturated calomel electrode (SCE), (E) Pt electrode, (F) oscilloscope, (G) board for data acquisition, (H) I/O connector block, and (I) Video camera.

regime is observed. Besides, for a total volume between 30 and 50 mL of solution the oscillations remain for between 2 and 5 hours.

A saturated calomel electrode (SCE) (Hg/Hg_2Cl_2, saturated KCl) was used as reference electrode and a platinum wire as working electrode. The platinum was covered with Parafilm to avoid contact with the acid solution and the free tip is immersed in the mercury so that there is continuous contact. It is convenient to put the SCE into a 6 M H_2SO_4 solution contained in a glass tube with a porous disc (salt bridge) in order to avoid the migration of Cl^- ions from the electrode electrolytic solution. The voltage–time curves can be measured with a digital oscilloscope (we used, for example, a TDS 520C Tektronix). The iron and platinum wires were from Aldrich with a purity of 99.9 %. It is recommend that this work be carried out in a ventilated area because of harmful Hg vapors. The setup is depicted in Figure 2.

To make a quantitative analysis, the oscillatory dynamics can be followed by a computerized analysis of voltage (in our case the signals were acquired with a National Instruments Lab-PC-1200/AI analog-to-digital converter board. This allowed us to take data every 500 μs). Then the 2.0-mm diameter iron wire with pointed tip was positioned at the periphery of the mercury drop. This triggers sustained oscillations of the mercury body, as it alternately makes and breaks contact with the mercury. This movement persists for around two hours until oscillations are extinguished. The oscillations were recorded using a Video Hi8 recorder, Sony model CCD-TR330.

Mechanism

In the geometry just described the motion of the Hg is relatively unconstrained and oscillations can occur in several modes. At the beginning, there is a complex motion as is illustrated in the sequence from 8 to 35 s shown in Figure 3, where pointed stars and concentric modes are seen (the authors have also reported other modes such as pentagons and hexagons [11]). It was recognized early on (and shown in reference 3) that the oscillations in acid medium originate from oxidation of the mercury surface followed by reduction back to mercury. In this process a film of mercury(I) sulfate is formed on the mercury surface, which affects the surface tension. In fact, it is observed that a film of sulfate (white color) is created on the surface of the metallic Hg.

The potential of the mercury shows irregular oscillations for approximately 25 min, then a period-1 oscillation develops, followed by a period-3 and finally a period-2 oscillation. This is shown for each type of oscillations in Figure 4 for selected time intervals. The system spends different times in each period, which depend on the initial concentration of the oxidant. In the irregular (aperiodic) regime the potential was ca. –0.35 V while the mercury was in contact with the iron wire. As the contact was broken the potential rose steeply to about +0.38 V and then dropped again as contact is remade, completing a cycle (Figure 4a). For the period-one regime the potential remained at ca. – 0.38 V for approximately 0.08 s and the maximum is about +0.16 V for the interval shown in Figure 4b, but this amplitude decreases as time goes on. For example, it is in the range –0.40 V to –0.075 V when t = 96 min. For the other cases (Figures 4c and 4d), there are different maxima corresponding to the different peaks.

We start the description of the redox cycle considering that $[Ce^{IV}(SO_4)_3]^{2-}$ can react with metallic Hg (referred hereafter as Hg^0) according to the following reactions:

$$2[Ce^{IV}(SO_4)_3]^{2-} + 2Hg^0 \rightleftarrows Hg_2^{2+} + 2[Ce^{III}SO_4]^+ + 4SO_4^{2-}(aq) \tag{2a}$$

$$2[Ce^{IV}(SO_4)_3]^{2-} + 2Hg^0 \rightleftarrows Hg_2SO_4(\text{soluble}) + 2[Ce^{III}SO_4]^+ + 3SO_4^{2-}(aq) \tag{2b}$$

$$2[Ce^{IV}(SO_4)_3]^{2-} + 2Hg^0 \rightleftarrows Hg_2SO_4(\text{insoluble}) + 2[Ce^{III}SO_4]^+ + 3SO_4^{2-}(aq) \tag{2c}$$

Here Hg_2^{2+} is the free ion in dissolution, Hg_2SO_4(soluble) is the soluble molecular mercury(I) sulfate and Hg_2SO_4(insoluble) is the precipitated or insoluble mercury(I) sulfate (film).

The metallic Fe (denoted as Fe^0) can undergo the following reactions

$$Fe^0 + Hg_2^{2+} \rightleftarrows Fe^{2+}(aq) + 2Hg^0 \tag{3a}$$

$$Fe^0 + Hg_2SO_4(\text{soluble}) \rightleftarrows Fe^{2+}(aq) + 2Hg^0 + SO_4^{2-}(aq) \tag{3b}$$

$$Fe^0 + Hg_2SO_4(\text{insoluble}) \rightleftarrows Fe^{2+}(aq) + 2Hg^0 + SO_4^{2-}(aq) \tag{3c}$$

We have observed the film presence during the entire initial time interval, but at the end of that interval the film is not observable. The formation of the species Hg_2SO_4(soluble) allows the establishment of equilibrium between the free ionic mercury species in solution and the insoluble mercurous sulfate:

$$Hg_2^{2+} + SO_4^{2-} \rightleftarrows Hg_2SO_4(\text{soluble}) \rightleftarrows Hg_2SO_4(\text{insoluble}) \tag{4}$$

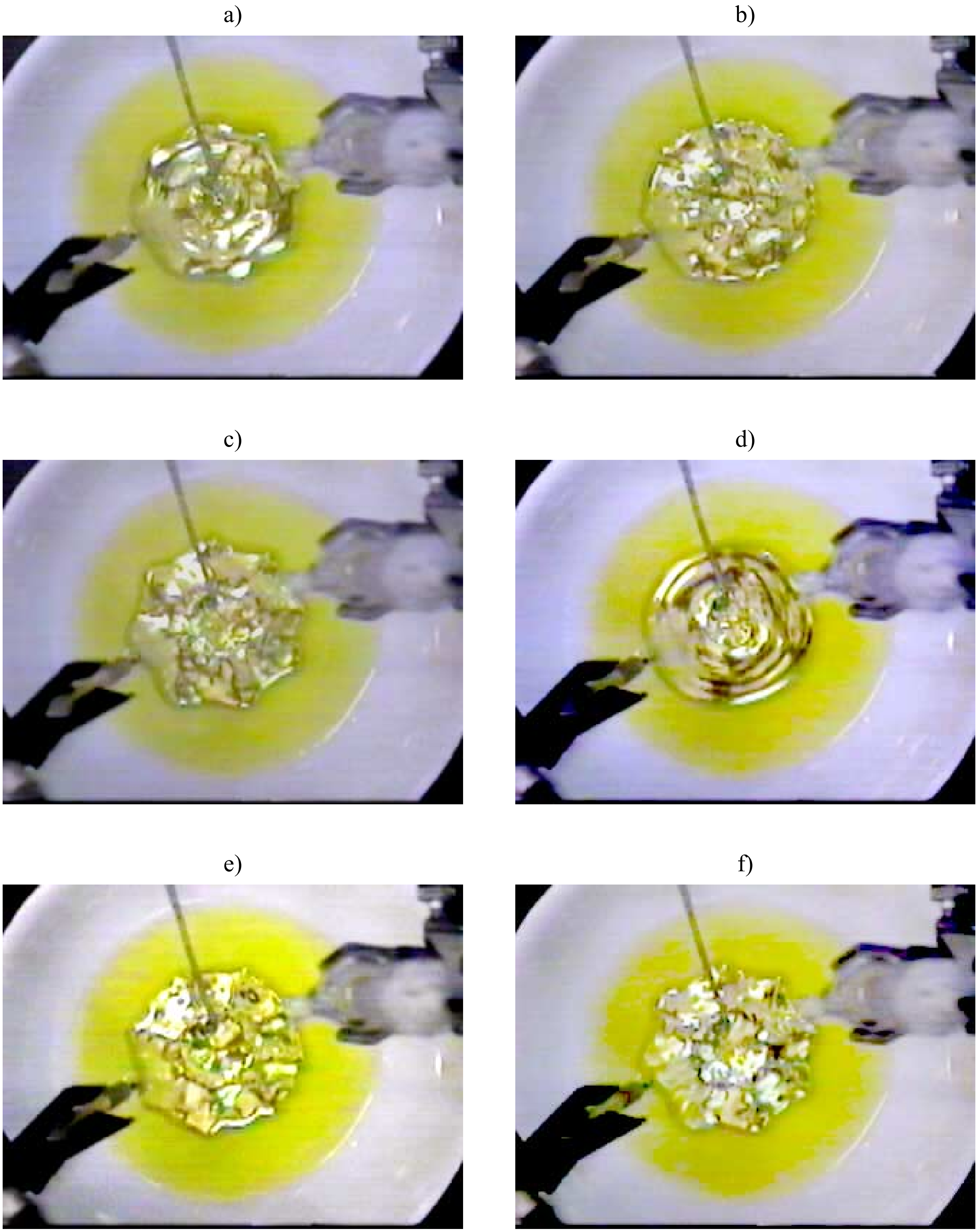

Figure 3. Oscillatory behavior of the MBH at the beginning of the experiment. The photographs were taken from the video recording and show the concentric-breathing and pointed-star modes of movement. The shots are in the interval 8 to 35 s: (a) 8 s, (b) 14 s, (c) 19 s, (d) 24 s, (e) 30 s, (f) 35 s.

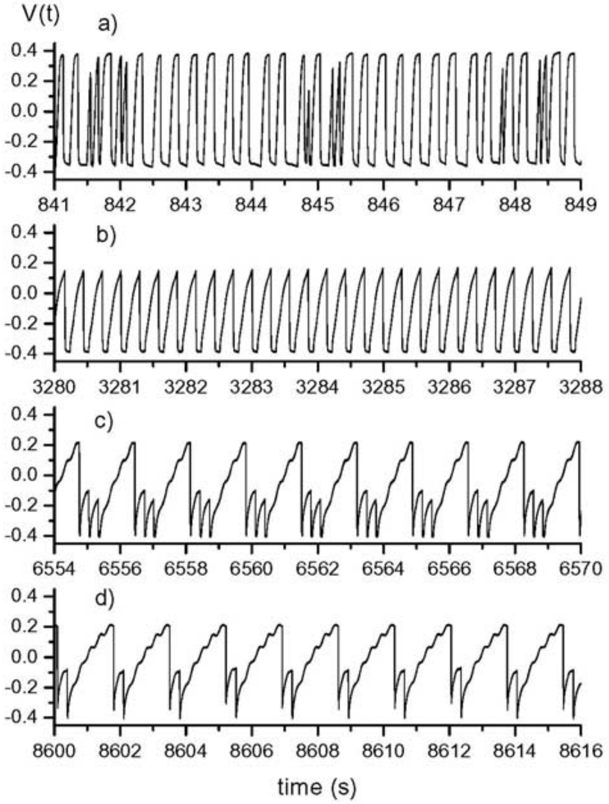

Figure 4. Time series for the potential of mercury, $V(t)$ versus t for different time intervals: (a) irregular oscillations, (b) period-one. (c) period-three, and (d) period-two.

When $[Ce^{IV}(SO_4)_3]^{2-}$ has been depleted, a second oxidant, the dissolved O_2, reacts with Hg^0 and the following three oxidation reactions can occur:

$$O_2 + 2Hg^0 + 4H^+ \rightleftarrows 2Hg^{2+} + 2H_2O \tag{5a}$$

$$Hg^{2+} + Hg^0 \rightleftarrows Hg_2^{2+} \tag{5b}$$

$$\begin{aligned} 2[Fe^{III}(SO_4)_2]^- + 2Hg^0 &\rightleftarrows 2Fe^{2+} \\ &+ Hg_2SO_4(\text{soluble}) + 3SO_4^{2-}(aq) \end{aligned} \tag{5c}$$

(Hg^{2+} is also denoted as mercury(II)) and the corresponding reduction reactions are

$$Fe^0 + Hg^{2+} \rightleftarrows Fe^{2+} + Hg^0 \tag{6a}$$

$$Fe^0 + Hg_2^{2+} \rightleftarrows Fe^{2+} + 2Hg^0 \tag{6b}$$

$$Fe^0 + Hg_2SO_4(\text{soluble}) \rightleftarrows Fe^{2+} + 2Hg^0 + SO_4^{2-} \tag{6c}$$

The Fe^{III} is produced in the reactions

$$Fe^0 + 2H^+ \rightleftarrows Fe^{2+} + H_2$$

$$2Fe^{2+} + Hg_2^{2+} + 4SO_4^{2-}{}_{(aq)} \rightleftarrows 2[Fe^{III}(SO_4)_2]^- + 2Hg^0$$

That all the above reactions can occur can in fact be deduced from a measurement of the oxidation-reduction potentials (as shown for example in Figure 4), which are in agreement with those calculated from the Nernst equation.

In conclusion, Hg^0 reacts with oxidizing agents according to their oxidizing strength. During the initial step the reaction with $[Ce^{IV}(SO_4)_3]^{2-}$ can produce the species Hg(I) and Hg(II) due to its oxidizing strength. In the first lapse, the only species formed is Hg(I) because there is competition between the formation of Hg(I) with slow kinetics and Hg(II) with fast kinetics; only the slow kinetics mechanism can be observed. When the $[Ce^{IV}(SO_4)_3]^{2-}$ is entirely depleted, Hg^0 reacts with the oxygen dissolved in the aqueous solution; then with Hg^{2+} as the concentration of this species increases, and finally with $[Fe^{III}(SO_4)_2]^-$. The proposed reactions to regenerate Hg^0 are the reductions of Hg(I) by the reducers Fe^0, Fe^{2+}, and H_2 When [Hg(II)] >> [Hg(I)] the reaction stops oscillating [11].

Nonlinear Dynamics

The phenomena such as oscillations, ignitions, and chemical patterns have become of great interest to the chemistry community in recent years. The conceptual and mathematical tools of the theory of dynamical dissipative systems have been used in the past [12] for analyzing models and experimental data of chemical systems.

A periodic regime is characterized by two parameters, the amplitude and the oscillation period. The time evolution or time variation $f(t)$ is called the time series. Especially the time series yield valuable information concerning the periodicity of the signal. A periodic function $f(t)$ can be represented as a superposition of its periodic components and the determination of their relative strengths is the spectral analysis. If $f(t)$ is periodic then the spectrum is a linear combination of a basic frequency. This linear combination is the Fourier series. If $f(t)$ is not periodic, the spectrum is expressed in terms of a continuum of frequencies. Such a spectral representation is the Fourier transform of $f(t)$. The modulus squared is called the power spectrum of $f(t)$.

For example, Figure 5 shows the power spectrum for each oscillatory record of Figure 4 obtained by Fourier transforming the time series. The power spectrum for the aperiodic oscillations of Figure 4a shows, instead of well-defined peaks, a broad-band structure as shown in Figure 5a. Once the periodic regime is established, at first the oscillations have small amplitude and basically a sinusoidal waveform (Figure 4b). This is reflected in the power spectrum, which shows a fundamental peak with a frequency at $\omega = 3.47$ Hz. As time goes on the period changes (Figures 4c and d) and more contributions in the power spectrum appear (Figures 5c and d). Using the L^S notation, where L is the number of large-amplitude excursions and S the number of small peaks in one complete period, we have states 1^0, 1^2, 1^1. The sequence of bifurcations is, thus, as follows: the system goes from one large peak (a 1^0 state) to a repeating unit consisting of one large and two small peaks (a 1^2 state) and subsequently to one large and one small peak (a 1^1 state).

The sustained oscillatory evolution projects on to the so-called phase plane, or variables space, to give a closed curve or limit cycle around which the trajectory moves. If we have data on just a single variable, as $V(t)$ in our case, we can construct an n-dimensional phase space in which the coordinates are $V(t)$, $V(t + \tau)$, $V(t + 2\tau)$, ..., $V(t + n\tau)$, where τ is the so-called delay time. The attractor constructed in this way is topologically equivalent to the attractor in the actual phase

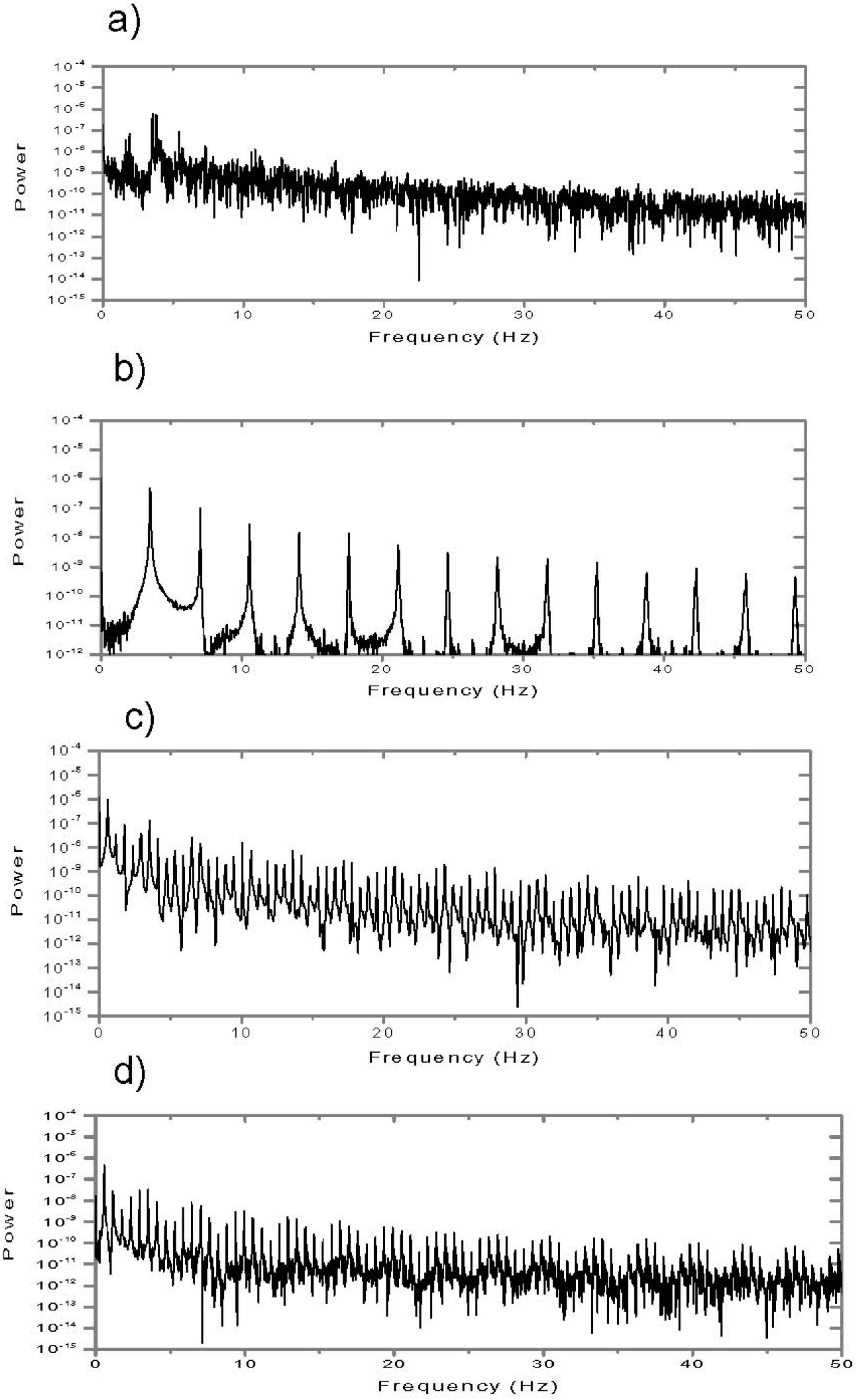

Figure 5. Power spectrum for each oscillatory record of Figure 4 obtained by Fourier transforming the time series.

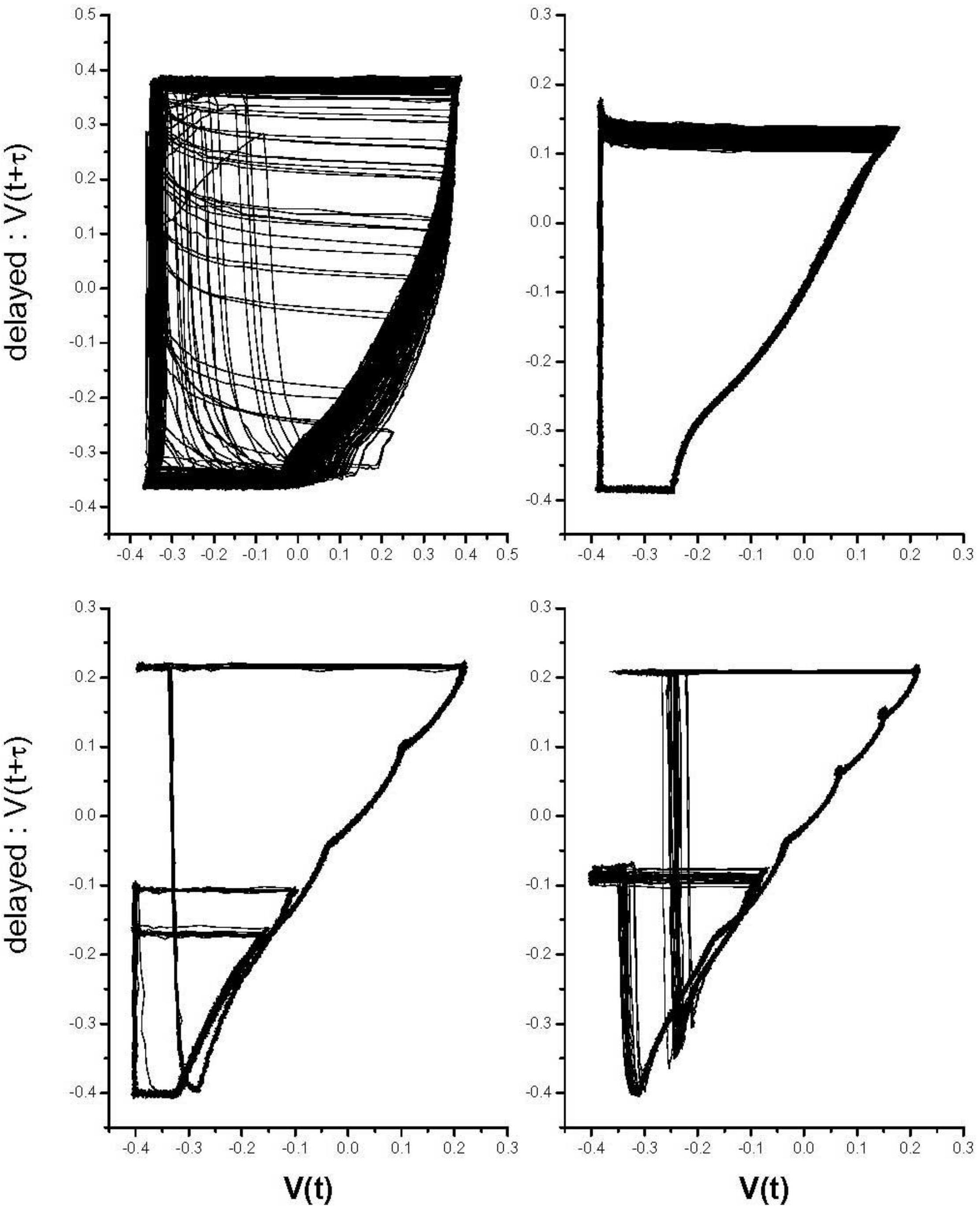

Figure 6. Reconstructed attractors shown in two-dimensional projection for the time series in Figure 4 using the delay method.

space [12]. This is another test for ordered structure: periodic attractors form closed curves, for the period-*n* responses closed circuits with *n* loops emerge. Performing this for the data corresponding to Figure 4 yields the attractors shown in Figure 6. The attractor corresponding to the aperiodic time series (Figure 4a) is also comprised of a series of circuits (there will indeed be an infinite number as it is shown in Figure 6a). As the reaction runs down, the system becomes periodic but the oscillatory behavior in each time interval is damped, which means that the experimental loop will consist in fact of many close loops. In this way Figure 6b shows the loop, which corresponds to the period-1 attractor. Figure 6c shows that the orbits corresponding to the time series of Figure 4c follow three loops. Figure 6d shows the attractor corresponding to the period-two response. It has to be noted that period-one, period-three and period-two limit cycles are all one-dimensional objects (lines), whereas a strange attractor corresponding to an aperiodic series has a dimension that is greater than one; it is a *fractal*.

Conclusion

The “Mercury Beating Heart” system can be used in the laboratory to introduce students to oscillations and aperiodicity in chemical reactions. As an example of a possible study we consider an acid aqueous solution with $[Ce^{IV}(SO_4)_3]^{2-}$ as oxidizing agent. Additional activities could be to verify that with the arrangement described above, the reaction presents an oscillatory behavior with the following oxidizing agents with a normal potential above 1.0 volts with respect to the normal hydrogen electrode (/NHE): H_2O_2, MnO_4^-, $Cr_2O_7^{2-}$, BrO_3^-, IO_3^- and VO_2^+ in H_2SO_4 solution. The setup described here is simple, and for a qualitative analysis the potential of mercury can be seen by using an oscilloscope, but to make a quantitative analysis the oscillatory dynamics must be followed by a computerized analysis of the voltage. The use of a video camera is also useful for classroom presentations. Besides, it allows taking still photographs from the tape as those shown in Figure 3.

From the electrochemical point of view, the pairs Hg(0)/Hg(I), Fe(0)/Fe(II) generate an electrical field that affects the surface tension and generates modes of oscillations. The mercury surface charge density changes alternately in the positive direction by an electrochemical oxidation and in the negative direction by contact with the corroding metal. The modes of oscillation are a function of the value of the global potential difference between the chemical reactions. We have considered possible oxidation–reduction reactions [11], eqs 2 through 6.

The system shows characteristics of nonlinear systems as bifurcations from aperiodic to (damped) periodic oscillations showing period-one, period-three, and period-two. From the time series the reconstructed attractors were plotted and the use of the Fourier transform allows testing for ordered structures within initial chaos. The periodic states all have simple waveforms 1^0, 1^2, 1^1, while the chaotic state is a mixture of different periodicities.

Acknowledgments. The present study was supported in part by DGAPA-IN100497, PAEP-005331, PAEP-012305 and CONACYT 32228-E.

Supporting Material. A recording of the first 60 s of the experiment (Figure 3) is available for download as a RealPlayer movie s00897020558b.rm (6.87MB).

References and Notes

1. Gray, P.; Scott S. K. *Chemical Oscillations and Instabilities;* Oxford University Press: Oxford, 1990.
2. Zhabotinsky, A. Dokl. Akad. Nauk. SSSR (Engl. Transl.) **1964,** 157, 392–395.
3. Lippmann, G. *Ann. Phys. (Leipzig)* **1873,** *149,* 546–561.
4. Hoff, H. E.; Geddes, L. A.; Valentinuzzi M. E.; Powell T. *Cardiovasc. Res. Bull.* **1971,** *IX* (3), 117–129; Powell, T.; Valentinuzzi M. E.; Hoff, H. E.; Geddes, L. A. *Experientia*, **1972,** *28,* 1009–1011.
5. Keizer, J.; Rock, P. A.; Lin, S. *J. Am. Chem. Soc.* **1979,** *101,* 5637–5649.
6. Avnir, D., *J. Chem. Educ.* **1989,** *66,* 211–212.
7. Olson, J.; Ursenbach, C.; Birss, V. I.; Laidlaw, W. G. *J. Phys. Chem.* **1989,** *93,* 8258–8263.
8. Smolin, S.; Imbihl, R., *J. Phys. Chem.* **1996,** *100,* 19055–19058.
9. Kim, C. W.; Yeo, I. H.; Paik, W. K.; *Electrochimica Acta* **1996,** *41,* 2829–2836.
10. Cotton, F. A.; Wilkinson G.; Murillo, C. A.; Bochmann, M. *Advanced Inorganic Chemistry;* Wiley & Sons: New York, 1999.
11. Castillo-Rojas, S.; González-Chávez, J. L.; Vicente L.; Burillo G. *J. Phys. Chem. A* **2001,** *105,* 8038–8045.
12. Epstein, I. R.; Pojman, J. A. *An Introduction to Nonlinear Chemical Dynamics;* Oxford University Press: New York, 1998.